

Methane Activation and Conversion to Higher Hydrocarbons on Supported Ruthenium

Jason N. Carstens and Alexis T. Bell

Chemical Sciences Division, Lawrence Berkeley National Laboratory and Department of Chemical Engineering, University of California, Berkeley, California 94720-1462

Received December 4, 1995; revised February 19, 1996; accepted February 26, 1996

The interaction of methane with silica-supported Ru has been investigated. Methane is found to undergo dissociative adsorption above 373 K. The preexponential factor for dissociative adsorption is 2.0×10^{-7} – 5.7×10^{-7} and the activation energy is 5.9–7.0 kcal/mol. Three types of carbon are formed, designated as C_{α} , C_{β} , and C_{γ} . The distribution among these species is dependent on the total carbon coverage and the length of time that the carbon has been aged at given temperature after deposition. Aging results in the conversion of C_{β} to C_{α} . The apparent activation energy for this process is 22 kcal/mol. Hydrogenation of the carbonaceous deposit produces methane and smaller quantities of ethane and propane. The distribution among these products depends on the surface coverage of carbon and the temperature of hydrogenation. Both the distribution of carbonaceous species present on the catalyst surface after dissociative adsorption of CH_4 and the distribution of alkanes formed upon isothermal hydrogenation of the carbonaceous deposit depend on whether or not the catalyst has been carburized. © 1996

Academic Press, Inc.

INTRODUCTION

The conversion of methane to higher molecular weight hydrocarbons remains as an important challenge for catalysis. Studies by van Santen and co-workers (1) have shown that methane can be activated thermally over supported Group VIII metals to produce carbonaceous species which can then be reacted with hydrogen to produce C_{2+} alkanes. Similar studies have been also reported by Amariglio *et al.* (2, 3) and by Solymosi and co-workers (4, 5). The dissociative adsorption of methane occurs above 373 K and produces three forms of carbon, referred to as C_{α} , C_{β} , and C_{γ} , which are distinguishable by the temperature at which they react with hydrogen. The yield of C_{2+} alkanes is sensitive to the temperature of hydrogenation, reaching a maximum at about 373 K. The formation of C_{2+} alkanes is hypothesized to proceed via processes similar to those occurring during Fischer–Tropsch synthesis. More recently, Goodman and co-workers have found that methane can be activated, as well, on Ru(0001) and Ru(1120) surfaces (6–8). High-resolution electron-energy loss spectroscopy

(HREELS) show three distinct forms of carbon, identified as methylidyne, CH, vinylidene, CCH_2 , and graphitic carbon on both surfaces. Ethylidyne, CCH_3 , was also observed on Ru(1120). Vinylidene was suggested to be a likely intermediate in the formation of ethane. Goodman and co-workers have also investigated the effects of methane dissociation temperature and carbon coverage on the yield of ethane produced by the hydrogenation of the carbonaceous species deposited onto Ru/SiO₂ (9).

The present investigation was undertaken to establish the effects of deposition conditions on the nature and reactivity of the carbonaceous species produced by the dissociative adsorption of methane on silica-supported Ru. Of particular interest were the influence of adsorption temperature and the coverage of carbonaceous species. The effects of aging on the distribution of the carbonaceous species was also investigated.

EXPERIMENTAL

A Ru/SiO₂ catalyst was prepared by incipient-wetness impregnation of Cab-O-Sil M5 (200 m²/g) with an aqueous solution of Ru(NO)(NO₃)₃. The impregnated support was dried under vacuum at 393 K overnight, pressed into a disk, and then crushed and sieved (35–60 mesh). The catalyst was then reduced in flowing H₂ for 5 h at 473 K, rinsed with boiling water to remove sodium impurities, and finally filtered and dried. The metal loading of the catalyst was 2.75 wt% Ru as determined by X-ray fluorescence spectroscopy. Hydrogen chemisorption at 298 K was used to measure the Ru dispersion using the assumption that the H:Ru ratio is 1:1. The dispersion calculated to be 18%, corresponding to 49.3 μmol of surface Ru per gram of catalyst. An identical value was obtained by temperature-programmed desorption of H₂ that had been previously adsorbed for 3 h at room temperature.

A 20-cm-long quartz microreactor with a 0.9-cm inside diameter quartz frit was used to support 0.30 g of catalyst. A thermocouple was placed into the catalyst bed for temperature measurements. The reactor was placed inside an electrically heated furnace controlled by a programmable

temperature controller (Omega Series CN-2010). All temperature-programmed experiments were conducted with a heating rate of 10 K/min.

Helium and hydrogen were supplied to the reactor from a gas manifold. The flow rate of each gas was controlled by a mass flow controller (Tylan FC-280). A six-way valve, located approximately 60 cm upstream of the catalyst bed was used to inject pulses of methane into the carrier gas. A premixed helium stream containing 10.4% CH₄ (Airco UHP, 99.999% minimum) was purified by passage through an oxygen adsorbent (Alltech) followed by a bed of molecular sieve (Linde 13X). H₂ (Airco, 99.999% minimum) was purified by passage through a De-Oxo catalytic hydrogen purifier (Engelhard Industries) to convert any oxygen impurity to water. The water was then removed by a molecular sieve trap immersed in liquid nitrogen. He (Airco, 99.999% minimum) was purified by a procedure similar to that used for CH₄, but with the trap immersed in liquid nitrogen.

The reactor effluent was monitored by a UTI Model 100C quadrupole mass spectrometer interfaced to a personal computer (Gateway 2000 4DX-33) for data acquisition. A portion of the effluent from the reactor was introduced through a leak valve (Granville-Phillips Series 203) into the vacuum chamber containing the mass spectrometer. Data points were taken every second during an isothermal hydrogenation step (see below) and every 5 s during a temperature-programmed experiment. The signal from the mass spectrometer was calibrated using an appropriate calibration gas.

Immediately downstream of the six-way valve used to inject methane pulses into the carrier gas was a four-way valve. This valve allowed the carrier gas, which normally flows through the reactor, to bypass the reactor and, hence, isolate the reactor from the rest of the flow system. In this way, injected methane could be passed either through the reactor or diverted via the bypass.

Experiments were performed with the catalyst pretreated in two different ways. In the first, the catalyst was reduced in a 60 cm³/min stream of 25% H₂ in He by ramping the temperature from room temperature to 898 K over a 1-h period. This sample is referred to as noncarburized. The second mode of pretreatment involved exposure of previously reduced Ru/SiO₂ to 20 pulses of methane (about 65 μmol) at 673 K. The catalyst was then left at that temperature for approximately 4 h under flowing He (60 cm³/min) and then for an additional 4 h under stagnant He. Finally the catalyst was cooled to room temperature and left overnight. The catalyst was then reduced following the same procedure used to prepare a noncarburized catalyst. The sample pretreated as described is referred to as carburized. Carburization was found to have no effect on the dispersion of Ru determined by temperature-programmed desorption of adsorbed H₂. Prior to each experiment, with either the noncarburized or the carburized catalyst, the catalyst was re-

duced in a stream of 25% H₂ in He flowing at 60 cm³/min by ramping the temperature from room temperature to 898 K over a 1-h period and then cooling to the desired reaction temperature.

RESULTS AND DISCUSSION

The dissociative adsorption of CH₄ on carburized and noncarburized Ru was investigated in the limit of small surface coverages (<0.1) by passing a single pulse of methane (3.2 μmol) over the catalyst. The amount of H₂ produced and the amount of carbon deposited were used as measures of the extent of dissociative adsorption. For a carrier gas flow rate of 60 cm³/s, each pulse had an average residence time in the catalyst bed of 0.75 s. Figure 1 shows Arrhenius plots for $(\Delta\theta/\Delta t)/Fa$ and $(\Delta N_{H_2}/\Delta t)/FA$, where $\Delta\theta$ and ΔN_{H_2} represent the differential change in carbon coverage and the moles of H₂ released in the time Δt that the catalyst has been exposed to CH₄, F is molar flux of CH₄, a is the surface area per mole of surface Ru sites, and A is the total surface area associated with surface Ru sites. Thus, the ordinate in Fig. 1 is the apparent sticking coefficient for the dissociative adsorption of methane, CH_{4,g} → CH_{x,s} + (4-x)/2H_{2,g}. For a given state of catalyst pretreatment, the sticking coefficient based on the measurement of carbon accumulation and that based on the measurement of hydrogen released fall along parallel lines. Moreover, for each type of measurement the data appear to be roughly independent of catalyst pretreatment. The difference between the two methods of measuring the sticking coefficient can be reconciled by taking a value of $x = 0.7$ for the H/C ratio of CH_{x,s}.

The activation energy for the dissociative adsorption of CH₄ on noncarburized Ru is 7.0 kcal/mol, whereas the corresponding barrier for carburized Ru is 5.9 kcal/mol. These values agree very closely with that reported for Ru/SiO₂ by

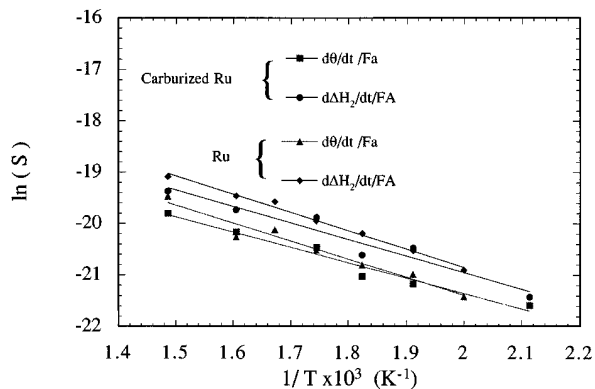


FIG. 1. An Arrhenius plot of the sticking coefficient for methane adsorption on noncarburized and carburized Ru. The sticking coefficient was determined from the amount of carbon deposited $(\Delta\theta/\Delta t)/Fa$ and from the amount of hydrogen produced $(\Delta H_2/\Delta t)/FA$ during the dissociative adsorption of methane.

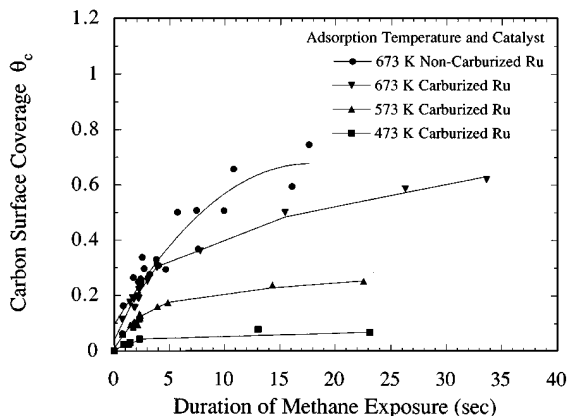


FIG. 2. The carbon surface coverage as a function of the number of pulses of 10.4% CH₄ exposed to the catalyst. Each pulse has a duration of about 0.75 s.

Koerts *et al.* (1), 6.2 kcal/mol, but are smaller than that reported by Wu and Goodman (7) for Ru(0001), 8.5 kcal/mol. Taking $a = 1.35 \times 10^3 \text{ cm}^2/\mu\text{mol Ru}$, and calculating F at the gas concentration in the pulse of CH₄, the value of s_0 , the preexponential factor for the sticking coefficient, is determined to be 5.8×10^{-7} for noncarburized Ru and 2.0×10^{-7} for carburized Ru. It is notable that these values are significantly smaller than the value of $s_0 = 9 \times 10^{-4}$ determined from the data of Wu and Goodman (7) for Ru(0001).

The accumulation of carbon on the catalyst surface as a function of cumulative exposure to a series of pulses (1–30 pulses) is presented in Fig. 2 for temperatures of 473, 573, and 673 K. Pulses of 10.4% CH₄ in He ($3.2 \mu\text{mol CH}_4/\text{pulse}$) were injected over a 2-min period. Each pulse had a residence time of 0.75 s. The time between pulses varied from as long as 1 min to as short as 2 s depending on the number of pulses introduced. The methane and hydrogen signals were monitored by the mass spectrometer and used to determine the amount of methane adsorbed dissociatively. The moles of carbon deposited on the catalyst was determined by integrating the methane signal observed during temperature-programmed reduction of the carbonaceous deposit in a stream containing 25% H₂ in He. The catalyst was heated at 10 K/min from room temperature to 898 K.

Figure 2 shows that for each temperature there is relatively rapid rise in the coverage at low exposures followed by a period of slower increase. At 673 K, the coverage by carbonaceous species is somewhat greater for the noncarburized than for the carburized sample, after a fixed exposure to CH₄. The H/C ratio of the carbonaceous deposit formed in these experiments remains roughly constant at the level of 0.7, independent of whether or not the catalyst is carburized, the temperature of carbon deposition, and the coverage by the carbonaceous species. This ratio is somewhat lower than what has been reported by Goodman and co-workers (6), who found that the dominant species

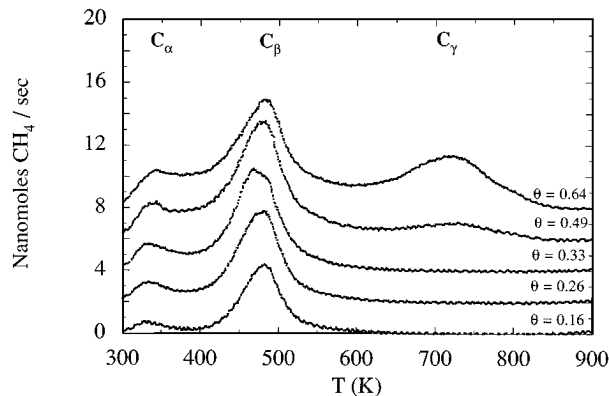


FIG. 3. TPSR spectra after dissociative adsorption of methane on noncarburized Ru at 673 K.

present on the Ru(0001) and Ru(1120) surfaces are CH and CCH₂.

The presence of different forms of carbon was established by temperature-programmed reduction of the carbonaceous deposit produced by the dissociative adsorption of methane. The procedure used for these experiments was identical to that used to obtain the data shown in Fig. 2. Figures 3 and 4 illustrate the rate of methane formation as a function of temperature for different initial coverages of carbon deposited on noncarburized and carburized Ru, respectively. In each case, the initial coverage by carbonaceous species is increased by increasing the number of pulses of CH₄ passed over the catalyst. Methane peaks appearing below 375 K are attributed to the reduction of C_α carbon, the peaks appearing between 375 and 625 K are attributed to the reduction of C_β carbon, and the peak above 625 K is attributed to the reduction of C_γ carbon, by analogy with what has been observed previously during the temperature-programmed reduction of carbonaceous species produced by dissociative adsorption of CO and by hydrogenation of CO (10–13). ¹³C NMR studies indicate that C_α is composed of single carbon atoms, C_β is composed

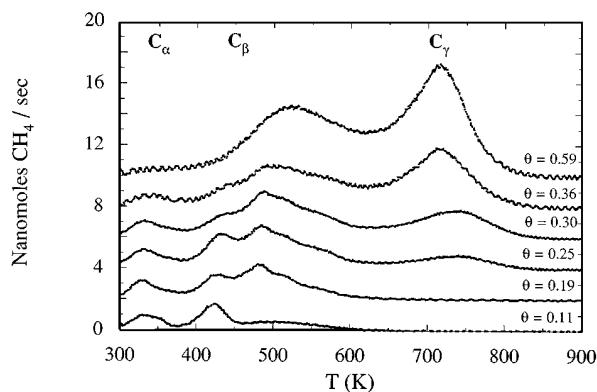


FIG. 4. TPSR spectra after dissociative adsorption of methane on carburized Ru at 673 K.

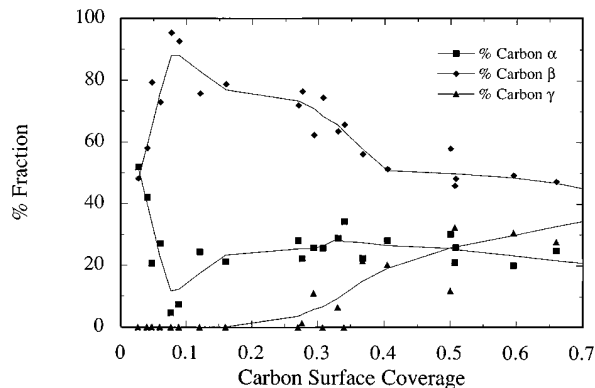


FIG. 5. The effect of surface coverage on the distribution of carbonaceous species deposited onto noncarburized Ru.

of $C_\gamma H_x$ species, and C_γ is composed of graphitic carbon (11, 12). The peaks in Figs. 3 and 4 associated with C_α can be further subcategorized into $C_{\alpha 1}$, which is designated as the carbon hydrogenated at temperatures < 298 K, and $C_{\alpha 2}$, which is designated as the carbon that is hydrogenated between 298 and 375 K. The peaks associated with C_β can be also be subcategorized into $C_{\beta 1}$, $C_{\beta 2}$, and $C_{\beta 3}$, with the peaks for $C_{\beta 1}$ and $C_{\beta 3}$ being observed only for the carburized catalyst (Fig. 4).

The observed differences in the TPD spectra for the noncarburized and carburized catalysts are directly attributable to aging of the carbonaceous overlayer in flowing He at 673 K. Aging in stagnant He was ineffective in changing the properties of the catalyst. During these experiments it was also observed that once carburized, the catalyst could not be restored to its noncarburized state by H_2 reduction at temperatures up to 898 K.

The distribution of C_α , C_β , and C_γ is shown in Figs. 5 and 6 as a function of the fractional coverage of the catalyst surface by carbonaceous species, θ . The data presented in these figures were obtained by deconvolution of the TPD peaks appearing in Figs. 3 and 4 and subsequent integration

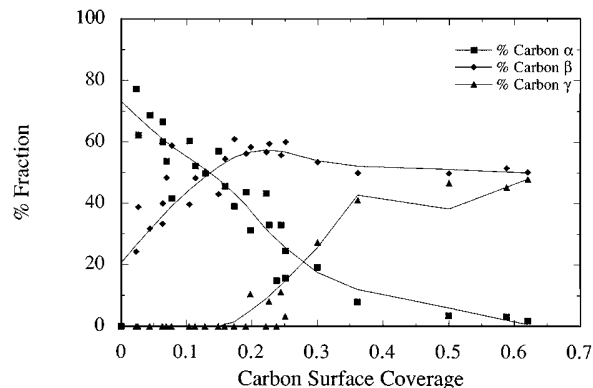


FIG. 6. The effect of surface coverage on the distribution of carbonaceous species deposited onto carburized Ru.

of the components. Inspection of Figs. 3 and 4 and Figs. 5 and 6 clearly shows that carburization of the catalyst has a strong effect on the distribution of carbonaceous species. For noncarburized Ru, the fraction of C_β is about 80% for small values of θ and then decreases to 45% as the value of θ increases to 0.7. The coverage by C_α remains nearly constant at 25%, independent of the value of θ , whereas the fraction of C_γ is initially zero and rises to about 35% once the value of θ increases above 0.3. For carburized Ru, the fraction of carbon present as C_α is about 80% for small values of θ and then decreases monotonically with increasing θ . The fraction of C_β is about 20% for θ close to zero. With increasing θ , the fraction of C_β rises to a maximum about 60%, and then decreases slightly. The fraction of C_γ is zero initially and then rises up to about 50%, for $\theta > 0.2$. The maximum value of θ in Fig. 4 is 0.6. In this case the only features observed are those for $C_{\beta 3}$ and C_γ . The distribution of C_α , C_β , and C_γ is very similar to that reported previously by Koerts *et al.* (1) for Ru/SiO₂.

The distribution of carbonaceous species on the catalyst surface changes when freshly deposited carbon is aged at constant temperature in He. These experiments were initiated by depositing a desired amount of carbon on the carburized catalyst surface by means of the pulse injection of CH_4 , after which the reactor was flushed with He and then isolated from the flow system. Aging of the carbonaceous deposit occurred in stagnant He at a fixed temperature for a proscribed time. Figure 7 shows TPR spectra for a freshly deposited overlayer, and after aging at 673 K for 1 and 2 h. As the aging time increases, the intensity of the $C_{\beta 1}$ peak decreases as the intensity for the C_γ peak increases monotonically.

A second set of aging experiments was designed to probe the conversion of C_β to C_α , and to determine whether or not the conversion of C_γ to either C_α or C_β occurs. For these experiments pulses of CH_4 were passed over the carburized catalyst at 673 K to produce an initial deposit of carbonaceous species. The catalyst was then reduced in a mixture

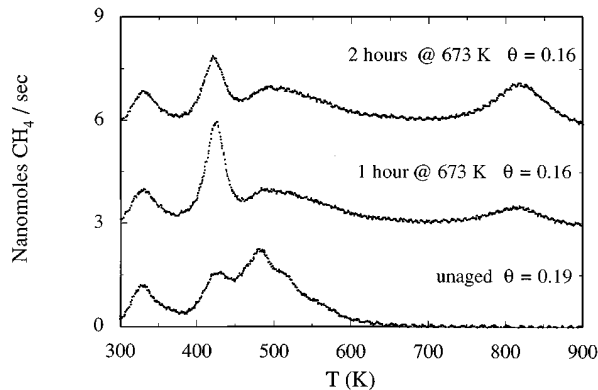


FIG. 7. TPRS spectra of methane adsorbed onto carburized Ru. Prior to TPRS the catalyst was aged for either 1 or 2 h at 673 K in stagnant He.

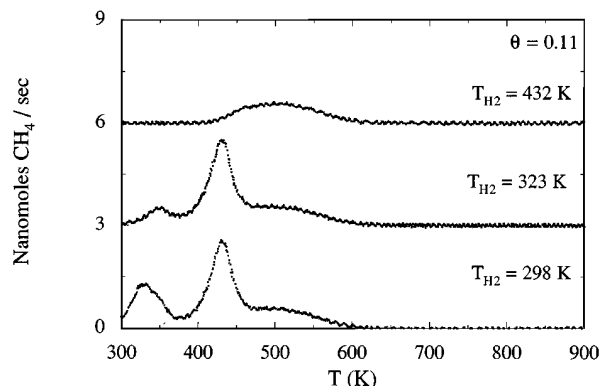


FIG. 8. TPSR spectra taken following isothermal hydrogenation at the indicated temperature of carbonaceous species deposited by methane adsorption onto carburized Ru. Methane was adsorbed at 673 K.

containing 25% H_2 in He at temperatures between 298 and 433 K for 5 min. The flow of H_2 was then stopped and the reactor was flushed with He ($45 \text{ cm}^3/\text{min}$) for 10 min to remove all traces of H_2 . The reactor was then brought to the desired aging temperature and isolated in an atmosphere of He. After aging the catalyst for a proscribed time, the reactor was again exposed to flowing He and the temperature was lowered to 298 K. Finally, a flow of H_2 in He was passed through the reactor and a TPR spectrum was recorded in the usual manner.

Figure 8 shows that increasing the temperature at which the isothermal reduction of the freshly deposited carbonaceous species is conducted results in the elimination of first the $C_{\alpha 2}$ and then the $C_{\beta 1}$ peaks from the TPR spectrum. Figure 9 shows TPSR spectra taken after the deposition of carbonaceous species at 673 K ($\theta = 0.2$) and subsequent isothermal reduction at 433 K. The TPR spectrum recorded after aging at 298 K for 24 h is identical to that recorded prior to aging, indicating that the carbonaceous deposit does not undergo changes at 298 K. For aging experiments

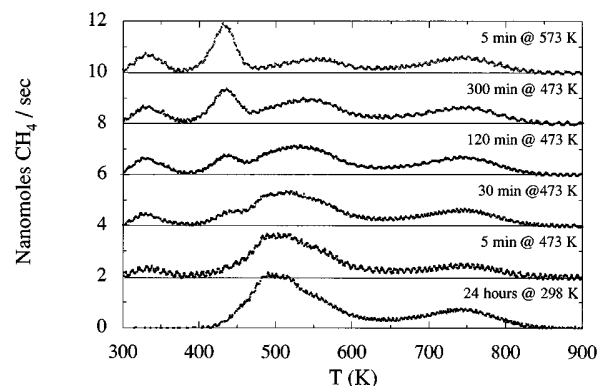


FIG. 9. TPSR spectra taken after aging the carbonaceous species deposited onto carburized Ru in stagnant He at the indicated temperature for the indicated length of time. Methane was adsorbed at 673 K.

conducted at 473 K, it is evident that as the deposit ages the carbonaceous species redistribute to produce $C_{\alpha 2}$ and $C_{\beta 1}$ at the expense of $C_{\beta 2}$. When aging is conducted at 573 K, the carbonaceous species redistribute in 5 min to the same extent as observed after 5 h at 473 K. While not shown, it was observed that the amount of $C_{\alpha 1}$ increased at a rate identical to that of $C_{\alpha 2}$ during aging at 473 and 573 K. The apparent activation energy for the conversion of $C_{\beta 2}$ to $C_{\alpha 2}$ and $C_{\beta 1}$ is 22 kcal/mol.

Ethane and smaller amounts of propane were observed, in addition to methane, during the isothermal hydrogenation of the carbonaceous deposit formed via the dissociative adsorption of methane. For these experiments the carbonaceous species were deposited onto the catalyst surface by the same method used to generate the data presented in Fig. 2. After cooling to the desired temperature, isothermal hydrogenation was initiated by switching from a flow of He to a flow containing 25% H_2 . The distribution of alkanes formed was found to be a function of both the coverage of the carbonaceous species and the temperature at which hydrogenation was conducted, as well as being a function of whether or not the catalyst had been carburized.

Figure 10 shows plots of the moles of methane and ethane produced upon hydrogenation of the carbonaceous layer at 298 K as a function of carbon coverage for both carburized and noncarburized Ru. The patterns of methane and ethane formation as a function of carbon coverage are radically different for noncarburized and carburized Ru. In the former case the moles of methane formed rises monotonically with increasing carbon coverage, and moles of ethane formed is always considerably lower than that of methane. By contrast, for carburized Ru the moles of methane and ethane formed pass through a maximum at a carbon coverage of about 0.15–0.20. Reference to Fig. 6 shows that at these coverages the fraction of carbon present as C_{β} is at a maximum. Careful examination of Fig. 10 reveals, further, that the formation of ethane is not observed below a threshold carbon coverage of 0.03. The ratio of ethane to methane obtained over carburized Ru is significantly higher than that obtained over noncarburized Ru.

The effects of hydrogenation temperature on the distribution of hydrocarbons formed is presented in Fig. 11. The initial coverage of carbon for these experiments is 0.25 for noncarburized Ru and 0.11 for carburized Ru. For noncarburized Ru the moles of methane, ethane, and propane formed all rise with increasing hydrogenation temperature and then pass through a maximum around 370 K. For carburized Ru increasing the hydrogenation temperature increases the yield of methane monotonically while the yield of ethane increases very slowly and reaches a maximum at about 370 K. A small amount of propane is observed when the hydrogenation temperature rises above 325 K. The fraction of propane increases with temperature up to a maximum at about 365 K, whereafter it decreases.

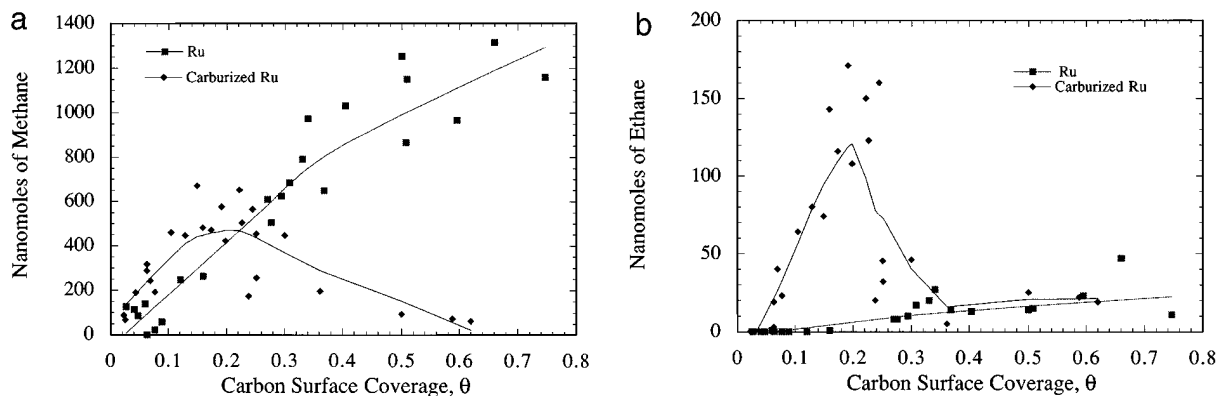
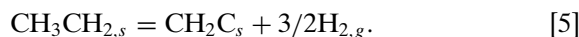
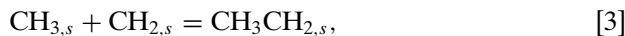
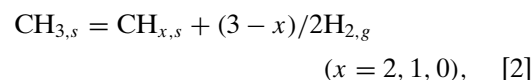
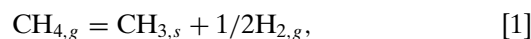


FIG. 10. The effect of carbon coverage on the yield of (a) methane and (b) ethane produced by isothermal hydrogenation of surface carbon at 298 K.

The temperature at which a maximum yield of C_{2+} products is observed is similar to that reported by Koerts *et al.* (1), 368 K.

The trends in ethane and propane formation observed in Fig. 11 can be attributed to two competing reactions. As the temperature increases, the rate of C_{2+} hydrocarbon formation increases until a temperature is reached above which the rate of ethane and propane hydrogenolysis becomes significant. Two experiments were performed to confirm this idea. In one experiment a 10% ethane in H_2 mixture was passed over the catalyst while the temperature was ramped at 10 K/min. Methane formation was observed above 425 K, indicating the onset of ethane hydrogenolysis. In the second experiment a 10% propane in H_2 stream was passed over the catalyst. Methane formation in this case was observed above 390 K. Virtually identical results were obtained with both the noncarburized and carburized catalysts, indicating that carburization does not affect the hydrogenolysis activity of the catalyst.

The overall chemistry of the interactions of methane with Ru can be summarized by the following steps:



The initial dissociative adsorption of methane is thought to produce $CH_{3,s}$, rather than species containing a lesser complement of hydrogen. BOC-MP calculations (14) demonstrate that the activation energy for the process $CH_{4,g} \rightarrow CH_{3,s} + H_s$ is 1 kcal/mol for Fe and 8 kcal/mol for Ni, bracketing the observed activation energy of 6.2–7.0 kcal/mol. The BOC-MP estimates of the activation energies for subsequent dehydrogenation of $CH_{3,s}$ to $CH_{x,s}$ ($x=2, 1, 0$) are 10–15 kcal/mol larger than those for the initial adsorption step. As a consequence, it is reasonable to expect that species such as CH_s and C_s derive from $CH_{3,s}$. While Goodman and co-workers have suggested that CH_2C_s is produced

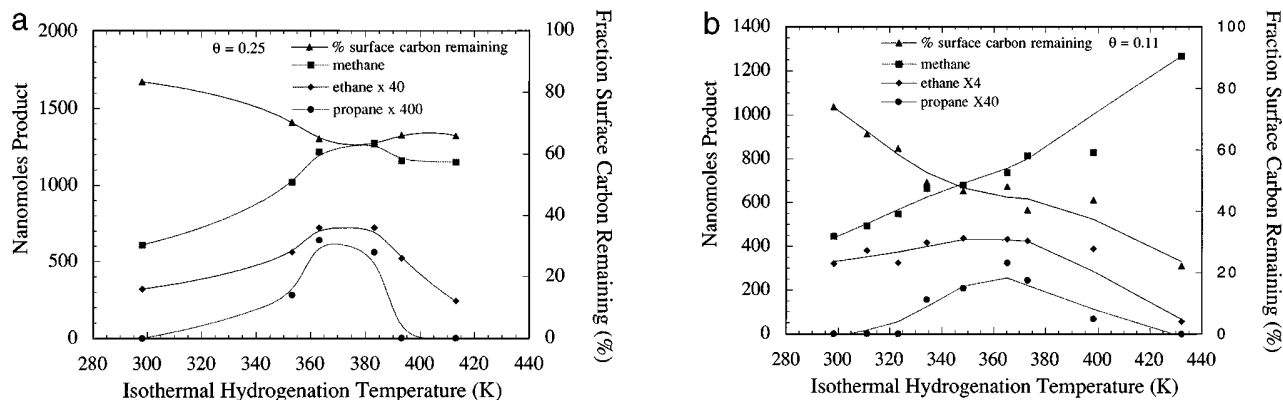


FIG. 11. The effect of temperature on the yield of methane, ethane, and propane produced by hydrogenation of surface carbon deposited on (a) noncarburized Ru and (b) carburized Ru.

via the process $\text{CH}_{2,s} + \text{C}_s \rightarrow \text{CH}_2\text{C}_s$, BOC-MP calculations (14) show that the activation energy for this process on Fe and Ni are 49 and 29 kcal/mol, respectively. A much more likely pathway to CH_2C_s is via reactions [3] and [5]. BOC-MP estimates of the activation barrier for the forward direction of reaction [3] are 20 and 6 kcal/mol for Fe and Ni, respectively, and the activation barriers for the subsequent dehydrogenation of CH_3CH_2 are less than 16 kcal/mol for both metals. The possibility that ethane is produced via reaction [2], $\text{CH}_{3,s} \rightarrow \text{CH}_3\text{CH}_{3,s}$, as proposed by Solymosi and co-workers, must also be considered as a possibility, since experimental results on Pd show that $\text{CH}_{3,s}$ groups will react to form ethane above 250 K (5). BOC-MP estimates of the activation barrier for the reverse of reaction [3] yield values of 18 and 24 kcal/mol for Fe and Ni, respectively (14). These values are close to the barrier height observed for the conversion of $\text{C}_{\beta 2}$ to $\text{C}_{\beta 1}$, $\text{C}_{\alpha 2}$, and $\text{C}_{\alpha 1}$, 22 kcal/mol, suggesting that the observed process involves depolymerization of alkyl species followed by rapid dehydrogenation of the resulting CH_x species to form C_α carbon.

It is evident from the data presented in Figs. 3 and 4 and in Figs. 10 and 11 that carburization of the catalyst alters both the distribution of carbonaceous species present on the catalyst surface after the catalyst is exposed to CH_4 and the distribution of alkanes formed when the carbonaceous species are reacted with H_2 under isothermal conditions. Carburization of the catalyst tends to increase the fraction of the carbonaceous deposit present in the form of C_α , but also that present as C_γ , at the expense of C_β , and to enhance the formation of C_{2+} alkanes during isothermal hydrogenation of the carbonaceous deposit. The origins of these effects are difficult to explain, since neither the dispersion, nor the activity of the catalyst for the dissociative adsorption of CH_4 are altered by carburization. Likewise, carburization has no effect on the hydrogenolysis activity of Ru. It is conceivable that during aging of the carbonaceous deposit in flowing He a part of the deposit loses hydrogen, forming small islands of graphite or graphitic precursors. Such species could, on the one hand, serve as hydrogen scavengers, thereby facilitating the transformation of $\text{CH}_{3,s}$ to C_s , and, on the other hand, as nuclei for the formation of C_γ . Further insights into the effects of carburization on the nature of the surface species formed upon dissociative adsorption of CH_4 must await their characterization by IR and NMR spectroscopy.

CONCLUSIONS

The dissociative adsorption of CH_4 on silica-supported Ru occurs with an apparent activation energy of 5.9–7.0 kcal/mol. The preexponential factor for the sticking coefficient for dissociative adsorption lies between 2.0×10^{-7}

and 5.7×10^{-7} . The carbonaceous species deposited on the catalyst surface exhibit a spectrum of reactivities with respect to hydrogen. Three broad classes of carbon, identified as C_α , C_β , and C_γ , are observed. C_α can be further classified into $\text{C}_{\alpha 1}$ and $\text{C}_{\alpha 2}$, and C_β can be further classified into $\text{C}_{\beta 1}$, $\text{C}_{\beta 2}$, and $\text{C}_{\beta 3}$. The distribution of these various forms of carbon depends on whether or not the catalyst has been carburized by exposing it to methane at 673 K and then aging the carbonaceous deposit in flowing He. On the carburized catalyst, with increasing carbon coverage the fraction of C_α decreases monotonically, the fraction of C_β passes through a maximum, and the fraction of C_γ increases monotonically. For the noncarburized catalyst, the fraction of C_α remains nearly constant while C_β initially increases to a maximum and then decreases. The distribution of carbon between C_α and C_β changes upon aging of the carbonaceous deposit, such that C_β is converted into C_α . The activation energy for this process is estimated to be 22 kcal/mol. No evidence is observed though for the conversion of C_γ to other forms of carbon. Hydrogenation of the carbonaceous deposit produces principally methane, together with smaller quantities of ethane and propane. The maximum yields of C_{2+} products coincides with the maximum in the surface coverage by C_β . The yield of C_{2+} hydrocarbons is an order of magnitude higher for the carburized catalyst than for the noncarburized catalyst.

ACKNOWLEDGMENT

This work supported by the Director of the Office of Basic Energy Sciences, Chemical Sciences Division, of the U.S. Department of Energy under Contract DE-AC03-76SF00098.

REFERENCES

1. Koerts, T., Deelen, M. J. A. G., van Santen, R. A., *J. Catal.* **138**, 101 (1992).
2. Belgued, M., Amariglio, H., Pareja, P., Ameriglio, A., and Saint-Just, J., *Catal. Today* **13**, 437 (1992).
3. Belgued, M., Pareja, A., Amariglio, A., and Amaraglio, H., *Nature* **352**, 789 (1991).
4. Solymosi, F., Erdohelyi, A., and Cserenyi, J., *Catal. Lett.* **16**, 399 (1992).
5. Solymosi, F., Erdohelyi, A., Cserenyi, J., and Felvegi, A., *J. Catal.* **147**, 272 (1994).
6. Lenz-Solomun, P., Wu, M., and Goodman, D. W., *Catal. Lett.* **25**, 75 (1994).
7. Wu, M., and Goodman, D. W., *Surf. Sci. Lett.* **306**, L529 (1994).
8. Wu, M., Xu, Q., and Goodman, D. W., *J. Phys. Chem.* **98**, 5104 (1994).
9. Koranne, M. M., Goodman, D. W., and Zajac, G. W., *Catal. Lett.* **30**, 219 (1995).
10. Winslow, P., and Bell, A. T., *J. Catal.* **86**, 158 (1984).
11. Duncan, T. M., Winslow, P., and Bell, A. T., *J. Catal.* **93**, 1 (1985).
12. Duncan, T. M., Reimer, J. A., Winslow, P., and Bell, A. T., *J. Catal.* **95**, 305 (1985).
13. Yokomizo, G. H., Louis, C., and Bell, A. T., *J. Catal.* **120**, 15 (1989).
14. Shustorovich, E., and Bell, A. T., *Surf. Sci.* **248**, 359 (1991).